Two Proposed Models for Face Recognition: Achieving High Accuracy and Speed with Artificial Intelligence

Hind Moutaz Al-Dabbas
Department of Computer Science, College of Education for Pure Science (Ibn Al-Haitham), Iraq | University of Baghdad, Iraq
hind.moutaz@ihcoedu.uobaghdad.edu.iq, cs.20.04@grad.uotechnology.edu.iq (corresponding author)

Raghad Abdulaali Azeez
Information Technology Unit, College of Education Ibn-Rushd for Human Sciences, Iraq | University of Baghdad, Iraq
raghad.azeez@ircoedu.uobaghdad.edu.iq

Akbas Ezaldeen Ali
Department of Computer Science, University of Technology, Iraq
akbas.e.ali@uotechnology.edu.iq

Received: 2 February 2024 | Revised: 11 February 2024 and 16 February 2024 | Accepted: 19 February 2024

 DOI: https://doi.org/10.48084/etasr.7002

ABSTRACT

In light of the development in computer science and modern technologies, the impersonation crime rate has increased. Consequently, face recognition technology and biometric systems have been employed for security purposes in a variety of applications including human-computer interaction, surveillance systems, etc. Building an advanced sophisticated model to tackle impersonation-related crimes is essential. This study proposes classification Machine Learning (ML) and Deep Learning (DL) models, utilizing Viola-Jones, Linear Discriminant Analysis (LDA), Mutual Information (MI), and Analysis of Variance (ANOVA) techniques. The two proposed facial classification systems are J48 with LDA feature extraction method as input, and a one-dimensional Convolutional Neural Network Hybrid Model (1D-CNNHM). The MUCT database was considered for training and evaluation. The performance, in terms of classification, of the J48 model reached 96.01% accuracy whereas the DL model that merged LDA with MI and ANOVA reached 100% accuracy. Comparing the proposed models with other works reflects that they are performing very well, with high accuracy and low processing time.

Keywords-ANOVA; CNN; face recognition; LDA; MI

I. INTRODUCTION

Face recognition technology and biometric systems have been employed for security purposes in various applications including Human Computer Interaction (HCI), surveillance systems, and facial animation and expression [1, 2]. Facial recognition software can recognize people from a collection of images or a video stream based on personal physical or behavioral traits, face, fingerprints, iris, and voice [3, 4]. Deep Learning (DL)-based face recognition has shown outstanding results [5, 6]. Convolutional Neural Networks (CNNs), one of the most often used types of deep neural networks in computer vision applications, demonstrate a key benefit of autonomous visual feature extraction [7]. CNNs typically have multiple convolutional layers, each with multiple filters of different sizes, allowing them to learn increasingly complex visual features as they process the input data [8, 9]. Several researchers have implemented face recognition systems with different classifiers like Machine Learning algorithms, such as Support Vector Machines (SVMs), K-Nearest Neighbor (KNN), Random Forest (RF), and Non-Negative Collaborative Representation-based Classifier (NCRC) using different feature extraction methods, namely Principal Component Analysis (PCA), Linear Discriminant Analysis (LDA), Gabor Wavelet's (GW), and Canonical Correlation Analysis (CCA) [10-16]. More recently, DL has been applied, which is believed to be more accurate and vital in face recognition. The DL techniques, such as GoogleNet, AlexNet, residual neural network (ResNet), and Visual Geometry Group Network (VGGNet and VGG-16) consider CNN architecture as the classifier [17-23].

DL methodology has relatively wider acceptance, so it was also considered in this research. Depending on J48 ML and the

deep one dimensional Convolutional Neural Network Hybrid Model (1D-CNNHM), two facial recognition techniques are proposed in this paper. Involving LDA feature extraction, which is combined with two feature selection methods, Mutual Information (MI) and Analysis of Variance (ANOVA), is considered an innovative step of this work. The objectives of this research are to propose advanced, high-accurate, and fast Artificial Intelligent (AI) models for facing impersonation crimes.

II. RELATED WORK

Authors in [10] proposed a face recognition system that depends on appearance-based features that focus on the entire face image rather than local facial features. The Viola-Jones face detection method was used. Feature extraction and dimension reduction methods were applied, using PCA and LDA. Square Euclidean Distance (SED) was employed to measure the distance between two images. Authors in [13] proposed an automatic face recognition system based on features focusing on the whole image as well as local-based features utilizing the Local Binary Pattern Histogram (LBPH), PCA, and LDA. In addition, the system deployed the ML algorithms PART and J48. The results displayed high accuracy for detection and feature extraction. Authors in [15] suggested a facial recognition system based on Multi-Scale Local Mapped Patterns (MSLMPs), using the Genetic Algorithm (GA) to optimize parameters and weight matrices. To deal with difficult databases like MUCT, this technique was established on the average gray levels of the images in the database. The results obtained for the database are superior and have high accuracy. Authors in [16] suggested the KNN algorithm for recognizing faces on an ARM processor. To reach the best k-value and create proper face recognition with a low-power processor, PCA and LDA were used for feature extraction. Authors in [20] proposed combining RFID cards with facial biometry based on DL to strengthen the safety of an e-payment organization through the use of the CASIA Face-V5 and MUCT datasets in order to assess and validate three DL face authentication models, namely Dlip, VGG-16, and ResNet-50. Combining RESNET-50 and PCA features yielded the greatest results, achieving 99.90% accuracy and 0.08% EERs on MUCT and 99.26% accuracy and 0.75% EERs on CASIA Face V5. Authors in [22] submitted a hybrid approach based on a Modified Local Binary Patterns (MLBPs) and Layered-Recurrent Neural Network (L-RNNs) for facial recognition. Utilizing the MUCT database and various ANN performance analyses, their hybrid technique yielded a classification rate of 98%.

III. MATERIALS AND METHODS

The MUCT database [24] was selected and applied in this research [13, 23]. Sample images from the MUCT database are illustrated in Figure 1. The selected database was divided into two sets, with 70% for training and 30% for testing. Every image in the database went through some preprocessing techniques. The image's facial region was detected and cropped using the Viola-Jones method [12]. Feature extraction and feature selection were applied [25]. Finally, the output classification was created by 1D-CNNHM. A preprocessing stage is implemented as the first phase, involving the conversion of color images to grayscale images, Histogram Equalization (HE), face detection, cropping, and resizing (Figure 2).

Fig. 1. Sample images from the MUCT database.

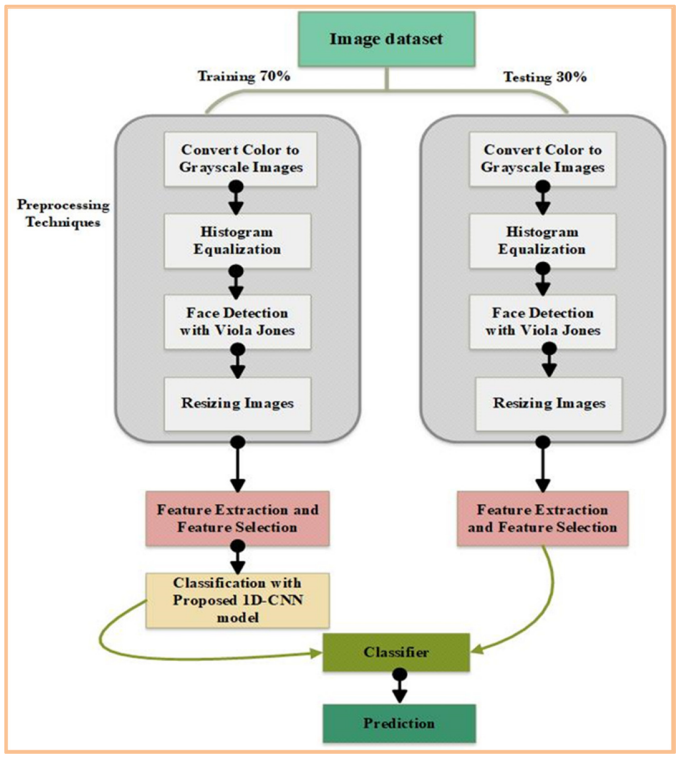

Fig. 2. The system methodology process.

A. Convert Color to Grayscale Images

The color models provide color data for each pixel in a particular image [18]. Grayscale image brightness was represented using an 8-bit value, whereas the color of a colored image's pixel is represented with a 24-bit value. The brightness in greyscale images spans from 0 to 255, with 0 intensity denoting black and 255 intensity denoting white [19, 20]. To convert the image into grayscale, the Red (R), Green (G), and Blue (B) colors should be averaged. Since each of the three hues has a unique wavelength and contributes differently to the creation of an image, the average must be calculated according to each color's contribution rather than just utilizing the average approach. This has been conducted by the luminosity method. The latter indicates that the contribution of the Red color must

be reduced, the contribution of the Green color must be increased, and the contribution of the Blue color must be placed between these two [26, 27]. Samples of the generated grayscale images are portrayed in Figure 3. The process of converting a colored to grayscale image is depicted in (1):

$$greyscale = (0.3 * R) + (0.5 * G) + (0.11 * B) \quad (1)$$

Fig. 3. Samples of grayscale images.

B. Histogram Equalization (HE)

HE is used to increase contrast in images. In order to improve low contrast images' quality and face recognition capabilities, it is common practice to distribute the most frequent intensity values evenly [27]. The image's dynamic range (contrast range) is altered as a result, making some crucial face features more noticeable [24]. Samples of images after HE are illustrated in Figure 4.

Fig. 4. Image samples after applying HE.

C. Face Detection with Viola Jones Algorithm

Viola-Jones algorithm was deployed for object detection due to its high accuracy and speed. Viola-Jones method consists of four concepts [23, 25], which are analyzed below.

1) Haar Features

The entire image is divided into M×M-sized squares or small windows. The characteristics of each window are selected separately. For face detection, three different feature types are commonly used: two-rectangle, three-rectangle, and four-rectangle features. The difference in the sums of the pixels within two rectangular sections is known as the "two-rectangle" characteristic. These rectangular areas are near to one another, either horizontally or vertically and have the same size and shape [23]. The three-rectangle feature adds the sum of the pixels in the middle rectangle to the sums of the pixels in the two outside rectangles. The difference between diagonal pairs of rectangles is computed in the four-rectangle feature, which is the final step [28]. These features are displayed in Figure 5.

Fig. 5. Haar features on the detected face.

2) Integral Image

An intermediate image representation known as an integral image was used to quickly calculate Haar-like features. Equation (2) shows the calculation formula. The integral image at position *x*, *y* contains the sum of the pixels above and to the left of (*x*, *y*) [29].

$$p(x,y) = \sum_{s=1}^{x} \sum_{t=1}^{y} I(s,t); 1 \le x \le M, 1 \le y \le M \quad (2)$$

where *p* denotes the integral image and *I* the original image.

3) Adaptive Boosting (Adaboost)

The Adaboost algorithm shrinks the size of a large set of features by removing pointless ones [30]. This method can replace thousands of features with hundreds or less. Such features are referred to as weak classifiers [26, 31].

4) Cascading

The discovered faces must proceed through a number of cascaded phases before finding the positive windows [32]. A classifier is created for each stage utilizing a few features. Every level after that adds more features, increasing the complexity of the classifier. Every stage has the option of rejecting or moving on to the next within the discovered region. Therefore, only the area that successfully completes all stages is categorized as a face [29]. After the Viola-Jones method was used, the images were in different sizes, so each image was resized employing bicubic interpolation into 100×100 size and then was cropped. The samples of the images after resizing and cropping are presented in Figure 6.

Fig. 6. Images after resizing and cropping.

Bicubic interpolation is an ideal method. It would also be a good option if quality was an issue. With bicubic interpolation, a pixel's 16 nearest neighbors are taken into account [34]. The intensity value assigned to point (*x*,*y*) is determined by:

$$v(x,y) = \sum_{i-0}^{3} \sum_{j=0}^{3} a_{ij} x^i y^j \quad (3)$$

D. Feature Extraction and Feature Selection

In order to reduce the complexity of space and time required for the proposed system model, the discriminative power of ANOVA and the thorough relationship assessment of MI with LDA feature extraction were combined. LDA was

merged with different percentage cases (5%, 10%, 15%, and 20%) of two feature selection methods, MI and ANOVA. It is possible to minimize the complexity of the space and the time needed for the proposed models by identifying the most pertinent features that have the most significant impact on the goal variable. This integration may improve model performance while reducing the drawbacks of each technique [35].

1) LDA Feature Extraction

The input data are transformed into a set of features during feature extraction, and the resultant reduced representation retains the majority of the pertinent data from the original data. LDA is a method of supervised linear dimensionality reduction that seeks for the subspace that distinguishes the most effective among several classes. The objective of LDA is to select an optimal solution vector as the best projection direction based on the Fisher criterion function and consider it not sensitive to light. The main LDA steps are [33]:

- Take samples for class-1 and class-2
- Calculate the class-1 and class-2 means as Mu1 and Mu2.
- Create class-1 and class-2 covariance matrices, denoted as C1 and C2, respectively.
- Compute the within-class scatter matrix

$$S_w = C1 + C2 \quad (4)$$

- Compute the between-class scatter matrix depending on the classes means:

$$S_B = (\mathrm{Mu1} - \mathrm{Mu2}) * (\mathrm{Mu1} - \mathrm{Mu2}) \quad (5)$$

- Compute all the class means.
- The basic eigenvalue problem is then solved by the LDA scheme in (6) and (7):

$$S_w^{-1} S_B W = \lambda \mathrm{W} \quad (6)$$

$$W = \mathrm{eig}(S_w^{-1} S_B) \quad (7)$$

where W is the projection vector.

2) ANOVA Feature Selection

ANOVA is a group of statistical models and associated estimation methods, which are used to evaluate variances in means [36]. The *f ratio* of the class-to-class variance over the within-class variance is the value determined by the ANOVA equations. A class separation indicator is provided by the size of the *f ratio* [28]. Data are preserved as features during retention times that result in an *f ratio* larger than a predetermined threshold, while the rest of the data are deleted [37]. The variance between classes is calculated by:

$$\sigma_{C1}^2 = \frac{\sum(\bar{x}_i - \bar{x})^2 n_i}{(k-1)} \quad (8)$$

where $\bar{x}_i$ is the mean of the i^{th} class, $\bar{x}$ stands for the mean, n_i is the number of measurements in the i^{th} class, N is the total sample size of the group, and k is the group number. The within-class variance is computed by:

$$\sigma_{err}^2 = \frac{\sum\sum(x_{ij} - \bar{x})^2 - (\sum(\bar{x}_i - \bar{x})^2 n_i}{(N-k)} \quad (9)$$

where x_{ij} is the j^{th} class's i^{th} measurement. The ratio of the two variances in (10) is used to generate the ANOVA *f ratio*:

$$f\ ratio\ \frac{\sigma_{C1}^2}{\sigma_{err}^2} \quad (10)$$

3) Mutual Information (MI) Feature Selection

MI is a measure of how much knowledge one random variable has about another [39]. This concept can be used to measure how relevant a feature subset is in relation to the output vector *C*, which is helpful in the context of feature selection. The MI is described by [38]:

$$\mathrm{MI}(x, y) = \sum_{i=1}^{n}\sum_{j=1}^{n} p(x((i), y(j)).\log\left(\frac{p(x((i), y(j))}{p(x(i)).p(y(j))}\right) \quad (11)$$

where MI is zero when *x* and *y* are statically independent, i.e. $p(x((i), y(j)) = p(x(i)).p(y(j))$. Considering two random variables *x* and *y*, their joint probability density function is $p(x((i), y(j))$.

E. ML Classification Model with J48 Decision Tree

ML research places a lot of emphasis on developing software that can automatically recognize complicated patterns and draw conclusions from data. This algorithm creates the rules for the target variable's prediction. The properties of J48 are accounting for missing values, Decision Tree (DT) pruning, continuous attribute value ranges, and derivation of rules. The objective is progressively generalization of a DT until it gains equilibrium of flexibility and accuracy. The output of this process is a DT classifier where each node represents a decision based on the selected attribute, and leaf nodes are labeled with class labels. Algorithm 1 displays the steps of J48 algorithm [36].

```
Algorithm 1: Steps of J48 Algorithm
Input: Features extracted by LDA
Output: Classifier
Processing steps:
Step 1: The leaf is labeled with a similar
class if the instances belong to the same
class.
Step 2: For each attribute, the potential
data will be generated and the gain in the
data will be derived from the test on the
attribute.
Step 3: The best attribute will be chosen
according to the current selection
parameter
```

F. Architecture of 1D-CNNHM

CNNs were considered for identification and classification. Filters, kernels, or neurons that can learn their weights, parameters, and biases make up CNNs [39, 40]. Each filter receives certain inputs, performs convolution, and then, if desired, adds nonlinearity [41, 42]. The structure of a CNN consists of convolutional, pooling, rectified linear unit (ReLU),

and fully connected layers [43]. The proposed 1D-CNNHM is built in 27 layers which include: 9 convolutional layers for 1D feature extraction, 6 Max-pooling 1D layers, 8 LeakyRelu layers for its ability to speed up the training of the model by reducing the slop for the negative feature values, 3 fully connected layers for collecting, and 1 flatten layer which flattens the output of the preceding layers into a single vector that can be the input for the following stage. This hybrid model produces higher predictive performance when compared to the traditional DL models. Each layer is presented with its filters, kernel size, strides (i.e. number of steps), and padding (refers to the amount of pixels added to an image when it is being processed by the kernel of a CNN). The total number of epochs is 100 and the batch size is 64. Adam learning optimizer with learning rate equal to 0.001 was employed. The model architecture is presented in Algorithm 2. The detailed layers of the proposed 1D-CNNHM architecture are depicted in Figure 7, in which K is the kernel size, F is the filter size, P is the pool size, and S is number of strides.

```
Algorithm 2: The architecture of the
proposed 1D-CNNHM
Input: Features of images
Output: 1D-CNNHM with optimum weights
Steps
Begin
Step 1: Add block 1
            Conv1D with (F=16, K=3, S=1)
            MaxPooling1D with (P=1, S=1)
            LeakyReLU with (alpha=0.3)
Step 2: Add block 2
            Conv1D with (F=32, K=3, S=1)
            MaxPooling1D with (P=1, S=1)
            LeakyReLU with (alpha=0.3)
Step 3: Add block 3
            Conv1D with (F=64, K=3, S=1)
            MaxPooling1D with (P=1, S=1)
            LeakyReLU with (alpha=0.3)
Step 4: Add block 4
             Conv1D with (F=64, K=3,
strides=1)
             MaxPooling1D with (P=1, S=1)
             LeakyReLU with (alpha=0.3)
             Dense with (F=64, activation
= "linear")
Step 5: Add block 5
             Conv1D with (F=32, K=3, S=1)
             MaxPooling1D with (P=1, S=1)
             LeakyReLU with (alpha=0.3)
Step 6: Add block 6
             Conv1D with (F=32, K=3,
strides=1)
             MaxPooling1D with (P=1, S=1)
             LeakyReLU with (alpha=0.3)
             Dense with (F=32, activation
= "linear")
Step 7: Add block 7
             Conv1D with (F=16, K=3, S=1)
             LeakyReLU with (alpha=0.3)
Step 8: Add block 8
             Conv1D with (F=16, K=3, S=1)
             LeakyReLU with (alpha=0.3)
Step 9: Conv1D with (F=485, K=3, S=1,
activation='linear')
Step 10: Flatten ()
Step 11: Dense with (F= 276, activation=
'softmax')
End
```

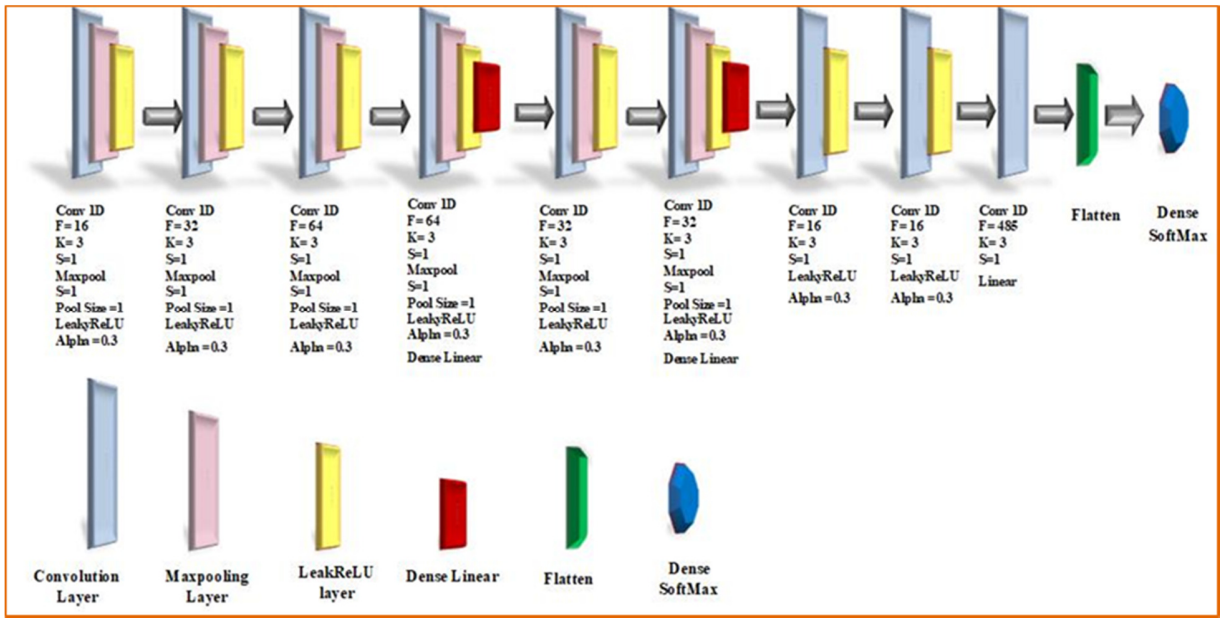

Fig. 7. Architecture layers of the proposed 1D-CNNHM.

G. Performance Measures

Various criteria, such as accuracy, precision, recall, and F1-measure were put into service for measuring the performance of the proposed hybrid algorithms [43, 44]. In (12)-(15), *TP* stands for True Positive, *TN* for True Negative, *FP* for False Positive, and *FN* for False Negative.

- Accuracy is the percentage of instances properly classified out of all those presented. It can be calculated by:

$$\text{Accuracy} = \frac{TN+TP}{TN+FP+FN+TP} \quad (12)$$

- Precision represents the correction ratio of predicting the positive results:

$$\text{Precision} = \frac{TP}{TP+FP} \quad (13)$$

- Recall is the correct prediction of the actual positive results:

$$\text{Recall} = \frac{TP}{TP+FN} \quad (14)$$

- F1-measure (score) is the harmonic mean of recall and precision:

$$F_1 = \frac{1}{\frac{1}{\text{Recall}}+\frac{1}{\text{Precision}}} = 2 * \frac{\text{Precision}*\text{Recall}}{\text{Precision}+\text{Recall}} \quad (15)$$

LDA applied with J48 ML achieved results with 96.01% accuracy, 96.03% precision, 95.45% recall, and 95.37% F1-measure, whereas applying 1D-CNNHM obtained results with 99.2% accuracy, and 99.3% precision, recall, and F1-measure. This means the 1D-CNNHM is considered more accurate in identifying patterns in image data compared to LDA with J48, and better at understanding and interpreting image data, proving to be them more effective for tasks like classification.

IV. RESULTS AND DISCUSSION

A. Time Performance

The time consuming result is considered to be good and low, as the processing time by using LDA feature extraction application only reached 5400 s for the whole training procedure. One epoch reached 55 s out of the 100 total epochs and 64 patch size. The training time of merging LDA feature extraction with MI and ANOVA feature selection reached 360 s. One epoch reached 3 s of 100 total epochs and 64 patch size.

B. Statistical Performance

LDA applied with J48 ML achieved results with 96.01% accuracy, 96.03% precision, 95.45% recall, and 95.37% F1-measure. 1D-CNNHM achieved results with 99.2% accuracy, and 99.3% for precision, recall, and F-measure. This means the 1D-CNNHM is considered more accurate in identifying patterns in image data compared to LDA with J48, and better at understanding and interpreting image data, making them more effective for classification tasks.

C. Merging Feature Performance

Merging 5% of ANOVA and MI with LDA obtained an impressive accuracy of 100%, while slightly reducing precision, recall, and F-measure to 99%. Merging 10% and 15% ANOVA, the performance remained highly competitive, with accuracy of 99.66% in both cases. Precision and recall remained consistently high, between 98.33% and 99.33%, while F1-measure ranged between 99% and 99.33%. At 20% merged features, the model was able to attain perfect performance metrics across the board, with 100% accuracy, precision, recall, and F-measure. These findings show the potential of combining features from ANOVA and MI at varying percentages to enhance predictive capability and optimize model efficiency, illustrating the efficacy of feature integration strategies in enhancing model performance and robustness. Table I summarizes the results. The outputs obtained by some previous related works using the MUCT database in several feature extraction and classification methods such as PCA, LDA, Gabor wavelet, and Haar-like features with different classifiers such as SVM, KNN, NCRC, J48, GA, and Euclidian distance, had accuracy ranging from 25.56% to 94.33% [10-16]. Other researchers used classifiers such as MLBP, L-RNN, CNN, Dlip deep, VGG-16, RESNET-50, and RESNET-101, with accuracy ranging from 91.87% to 98.55% [19-23]. The two proposed systems reached very good results with high accuracy and quick processing. The 1D-CNNHM is considered to perform better than J48. Table II illustrates the comparison between the proposed algorithms and some earlier relative works.

TABLE I. RESULTS OF PROPOSED SYSTEMS

Classifier	Accuracy	Precision	Recall	F1- score
LDA + J48 ML	96.01%	96.03%	95.45%	95.37%
LDA+1D-CNNHM	99.2%	99.3%	99.3%	99.3%
LDA+ 5% (ANOVA & MI) + 1D-CNNHM	100%	99%	99%	99%
LDA+ 10% (ANOVA & MI) + 1D-CNNHM	99.66%	98.33%	99%	99%
LDA+ 15% (ANOVA & MI) + 1D-CNNHM	99.66%	98.66%	99.33%	99.33%
LDA+ 20% (ANOVA & MI) + 1D-CNNHM	100%	100%	100%	100%

TABLE II. COMPARISON BETEEN PROPOSED SYSTEMS AND SOME PREVIOUS WORKS

Work	Feature extraction	Classifier	Accuracy
[11]	-	SVM, KNN, NCRC	25.56%, 27.87%, 77.78%
[14]	-	Random Forest SVM	83.3% 96.3%
[10]	PCA and LDA	Euclidean distance	87.5%
[16]	PCA and LDA	KNN	91.5%
[15]	MSLMP	GA	93.49%
[12]	Gabor Wavelets	SVM	93.70%
[13]	LDA	PART, J48	91.21% 94.33%
[21]	Counterfeit feature extraction	CNN with ELA	97.6%
[22]	MLBP	L-RNN with quasi-Newton back propagation	98%
[20]	PCA	Dlip deep model, VGG-16,	96.28% 99.64%
[19	Haar-like and LPPF	ResNet50, ResNet101	91.87% 98.55%.
Proposed	LDA	J48 ML	96.01%
Proposed	LDA with ANOVA and MI	1D-CNNHM	100%

V. CONCLUSIONS

High accuracy and faster performance models were proposed in this paper. LDA feature extraction method was deployed as the input of J48 machine learning model, and the novel 1D-CNNHM model, depending on LDA feature extraction with feature selection from MI and ANOVA was presented. MUCT database was considered for model training and validation. Through preprocessing techniques, the images are detected and cropped using the Viola-Jones algorithm, owing to its high degree of accuracy detection and speed. To evaluate the classification success of the suggested systems, a number of measures designed for evaluation performance including accuracy, precision, recall, and the F1-measure were utilized. Applying the LDA feature extraction with J48, the performance measure reached 96.01% accuracy, 96.03% precision, 95.45% recall, and 95.37% F1-measure, while applying LDA with 1D-CNN HM reached 99.2% accuracy, and 99.3% precision, recall, and f1-measure. When merging LDA feature extraction with different percentages of MI and ANOVA feature selection (5%, 10%, 15%, and 20%), perfect resulting performance of 100% accuracy, precision, recall, and the F1-measure was acquired for the 20% of merging features. Consumed time reached 55 s for 1 out of the 100 total epochs and 64 patch size. The time of merging the LDA feature extraction with MI and ANOVA feature selection reached 3 s for 1 out of the 100 total epochs and 64 patch size. Such findings are considered to be excellent when compared with previous works.

REFERENCES

[1] A. Y.Noori, S. H. Shaker, and R. A. Azeez, "3D scenes semantic segmentation using deep learning based Survey," *IOP Conference Series: Materials Science and Engineering*, vol. 928, no. 3, Aug. 2020, Art. no. 032083, https://doi.org/10.1088/1757-899X/928/3/032083.

[2] A. Azeez and Raghad, "Determination Efficient Classification Algorithm for Credit Card Owners: Comparative Study," *Engineering and Technology Journal*, vol. 39, no. 1B, pp. 21–29, Mar. 2021, https://doi.org/10.30684/etj.v39i1B.1577.

[3] N. H. Ali, M. E. Abdulmunem, and A. E. Ali, "Constructed model for micro-content recognition in lip reading based deep learning," *Bulletin of Electrical Engineering and Informatics*, vol. 10, no. 5, pp. 2557–2565, Oct. 2021, https://doi.org/10.11591/eei.v10i5.2927.

[4] W. Najah Abdullah and Y. Hussain Ali, "Face Retrieval Using Image Moments and Genetic Algorithm," *Engineering and Technology Journal*, vol. 34, no. 1B, pp. 160–171, Jan. 2016, https://doi.org/10.30684/etj.34.1B.18.

[5] H. Al-Dabbas and F. Mohammed, "The Effect of Wavelet Coefficient Reduction on Image Compression Using DWT and Daubechies Wavelet Transform," *Science International*, vol. 30, no. 5, pp. 757–762, Jan. 2018.

[6] N. A. Taha, Z. Qasim, A. Al-Saffar, and A. A. Abdullatif, "Steganography using dual tree complex wavelet transform with LSB indicator technique," *Periodicals of Engineering and Natural Sciences*, vol. 9, no. 2, pp. 1106–1114, Jun. 2021, https://doi.org/10.21533/pen.v9i2.2060.

[7] W. N. Abdullah, "Solving Job-Shop Scheduling Problem Using a Developed Particle Swarm Optimization Algorithm," *International Journal of Science and Research*, vol. 7, no. 1, pp. 1845–1848, 2015, https://doi.org/10.21275/ART20179752.

[8] F. B. Ibrahim and M. E. Abdulmunim, "Real Time Face Recognition System based Hybrid Method," *International Journal of Scientific Research & Management Studies*, vol. 4, no. 4, pp. 6–11, May 2018.

[9] A. H. Morad and H. M. Al-Dabbas, "Classification of Brain Tumor Area for MRI images," *Journal of Physics: Conference Series*, vol. 1660, no. 1, Aug. 2020, Art. no. 012059, https://doi.org/10.1088/1742-6596/1660/1/012059.

[10] N. H. Barnouti, S. S. M. Al-Dabbagh, W. E. Matti, and M. A. S. Naser, "Face Detection and Recognition Using Viola-Jones with PCA-LDA and Square Euclidean Distance," *International Journal of Advanced Computer Science and Applications*, vol. 7, no. 5, pp. 371–377, 2016.

[11] J. Zhou and B. Zhang, "Collaborative Representation Using Non-Negative Samples for Image Classification," *Sensors*, vol. 19, no. 11, Jan. 2019, Art. no. 2609, https://doi.org/10.3390/s19112609.

[12] J. A. C. Moreano and N. B. L. S. Palomino, "Efficient Technique for Facial Image Recognition With Support Vector Machines in 2D Images With Cross-validation in Matlab," *Wseas Transactions on Systems and Control*, vol. 15, pp. 175–183, May 2020, https://doi.org/10.37394/23203.2020.15.18.

[13] A. H. Rashed and M. H. Hamd, "Robust Detection and Recognition System based on Facial Extraction and Decision Tree," *Journal of Engineering and Sustainable Development*, vol. 25, no. 4, pp. 40–50, Jul. 2021, https://doi.org/10.31272/jeasd.25.4.4.

[14] R. Szmurlo and S. Osowski, "Ensemble of classifiers based on CNN for increasing generalization ability in face image recognition," *Bulletin of the Polish Academy of Sciences. Technical Sciences*, vol. 70, no. 3, 2022, Art. no. e141004, https://doi.org/10.24425/bpasts.2022.141004.

[15] E. M. Silva, M. Boaventura, I. A. G. Boaventura, and R. C. Contreras, "Face Recognition Using Local Mapped Pattern and Genetic Algorithms," in *International Conference on Pattern Recognition and Artificial Intelligence*, Union, NJ, USA, Dec. 2018, pp. 11–17, https://doi.org/10.1145/3243250.3243262.

[16] E. Setiawan and A. Muttaqin, "Implementation of K-Nearest Neightbors Face Recognition on Low-power Processor," *Telkomnika*, vol. 13, no. 3, pp. 949–954, Sep. 2015, https://doi.org/10.12928/telkomnika.v13i3.713.

[17] C. Szegedy *et al.*, "Going deeper with convolutions," in *IEEE Conference on Computer Vision and Pattern Recognition*, Boston, MA, USA, Jun. 2015, pp. 1–9, https://doi.org/10.1109/CVPR.2015.7298594.

[18] I. Alhakam and N. H. Salman, "An Improved Probability Density Function (PDF) for Face Skin Detection," *Iraqi Journal of Science*, vol. 63, no. 10, pp. 4460–4473, Oct. 2022, https://doi.org/10.24996/ijs.2022.63.10.31.

[19] S. O. Adeshina, H. Ibrahim, S. S. Teoh, and S. C. Hoo, "Custom Face Classification Model for Classroom Using Haar-Like and LBP Features with Their Performance Comparisons," *Electronics*, vol. 10, no. 2, Jan. 2021, Art. no. 102, https://doi.org/10.3390/electronics10020102.

[20] N. K. Benamara, M. Keche, M. Wellington, and Z. Munyaradzi, "Securing E-payment Systems by RFID and Deep Facial Biometry," in *1st International Conference on Artificial Intelligence and Data Analytics*, Riyadh, Saudi Arabia, Apr. 2021, pp. 151–157, https://doi.org/10.1109/CAIDA51941.2021.9425175.

[21] W. Zhang and C. Zhao, "Exposing Face-Swap Images Based on Deep Learning and ELA Detection," *Proceedings*, vol. 46, no. 1, 2019, Art. no. 29, https://doi.org/10.3390/ecea-5-06684.

[22] A. Al-Qaisi, M. Altarawneh, A. ElSaid, and Z. Al Qadi, "A Hybrid Method of Face Feature Extraction, Classification Based on MLBP and Layered- Recurrent Network," *Traitement du Signal*, vol. 37, pp. 555–561, Oct. 2020, https://doi.org/10.18280/ts.370402.

[23] H. M. Al-Dabbas, R. A. Azeez, and A. E. Ali, "Machine Learning Approach for Facial Image Detection System," *Iraqi Journal of Science*, vol. 64, no. 10, pp. 6328–6341, Oct. 2023, https://doi.org/10.24996/ijs.2023.64.10.44.

[24] "The MUCT Face Database." http://www.milbo.org/muct/.

[25] F. G. Mohammed and H. M. Al-Dabbas, "Application of WDR Technique with different Wavelet Codecs for Image Compression," *Iraqi Journal of Science*, vol. 59, no. 4B, pp. 2128–2134, Nov. 2018, https://doi.org/10.24996/ijs.2018.59.4B.18.

[26] A. Salim Jamil, R. Azeez, and N. Hassan, "An Image Feature Extraction to Generate a Key for Encryption in Cyber Security Medical Environments," *International Journal of Online and Biomedical*

Engineering, vol. 19, no. 1, pp. 93–106, Jan. 2023, https://doi.org/10.3991/ijoe.v19i01.36901.

[27] J. M. AL-Tuwaijari, S. I. Mohammed, and M. A. B. Rahem, "Performance Evaluation of Face Image Recognition Based Voila–Joins with SVM," *Iraqi Journal of Information Technology*, vol. 9, no. 1, pp. 48–64, 2018.

[28] H. Alamri, E. Alshanbari, S. Alotaibi, and M. Alghamdi, "Face Recognition and Gender Detection Using SIFT Feature Extraction, LBPH, and SVM," *Engineering, Technology & Applied Science Research*, vol. 12, no. 2, pp. 8296–8299, Apr. 2022, https://doi.org/10.48084/etasr.4735.

[29] M. N. Chaudhari, M. Deshmukh, G. Ramrakhiani, and R. Parvatikar, "Face Detection Using Viola Jones Algorithm and Neural Networks," in *Fourth International Conference on Computing Communication Control and Automation*, Pune, India, Aug. 2018, pp. 1–6, https://doi.org/10.1109/ICCUBEA.2018.8697768.

[30] Y. Said, M. Barr, and H. E. Ahmed, "Design of a Face Recognition System based on Convolutional Neural Network (CNN)," *Engineering, Technology & Applied Science Research*, vol. 10, no. 3, pp. 5608–5612, Jun. 2020, https://doi.org/10.48084/etasr.3490.

[31] M. K. Dabhi and B. K. Pancholi, "Face Detection System Based on Viola - Jones Algorithm," *International Journal of Science and Research*, vol. 5, no. 4, pp. 62–64, 2013.

[32] M. E. Abdulmunem and F. B. Ibrahim, "Design of an Efficient Face Recognition Algorithm based on Hybrid Method of Eigen Faces and Gabor Filter," *Iraqi Journal of Science*, vol. 57, no. 3B, pp. 2102–2110, 2016.

[33] H. Santoso and R. Pulungan, "A Parallel Architecture for Multiple-Face Detection Technique Using AdaBoost Algorithm and Haar Cascade," in *Information Systems International Conference*, Bali, Indonesia, Dec. 2013, pp. 592–597.

[34] N. Singhal, V. Ganganwar, M. Yadav, A. Chauhan, M. Jakhar, and K. Sharma, "Comparative study of machine learning and deep learning algorithm for face recognition," *Jordanian Journal of Computers and Information Technology*, vol. 7, no. 3, pp. 313–325, Sep. 2021, https://doi.org/10.5455/jjcit.71-1624859356.

[35] Y. Aliyari Ghassabeh, F. Rudzicz, and H. A. Moghaddam, "Fast incremental LDA feature extraction," *Pattern Recognition*, vol. 48, no. 6, pp. 1999–2012, Jun. 2015, https://doi.org/10.1016/j.patcog.2014.12.012.

[36] E. A. Khorsheed and Z. A. Nayef, "Face Recognition Algorithms: A Review," *Academic Journal of Nawroz University*, vol. 11, no. 3, pp. 202–207, Aug. 2022, https://doi.org/10.25007/ajnu.v11n3a1432.

[37] H. M. Al-Dabbas, R. A. Azeez, and A. E. Ali, "Digital Watermarking, Methodology, Techniques, and Attacks: A Review," *Iraqi Journal of Science*, vol. 64, no. 8, pp. 4169–4186, Aug. 2023, https://doi.org/10.24996/ijs.2023.64.8.37.

[38] K. J. Johnson and R. E. Synovec, "Pattern recognition of jet fuels: comprehensive GC×GC with ANOVA-based feature selection and principal component analysis," *Chemometrics and Intelligent Laboratory Systems*, vol. 60, no. 1, pp. 225–237, Jan. 2002, https://doi.org/10.1016/S0169-7439(01)00198-8.

[39] S. Shakeela, N. S. Shankar, P. M. Reddy, T. K. Tulasi, and M. M. Koneru, "Optimal Ensemble Learning Based on Distinctive Feature Selection by Univariate ANOVA-F Statistics for IDS," *International Journal of Electronics and Telecommunications*, no. Vol. 67, No. 2, pp. 267–275, 2021, https://doi.org/10.24425/ijet.2021.135975.

[40] Y. H. Ali and W. N. Abdullah, "A Survey of Similarity Measures in Web Image Search," *International Journal of Emerging Trends & Technology in Computer Science*, vol. 4, no. 4, pp. 191–196, 2015.

[41] H. M. Al-Dabbas, R. A. Azeez, and A. E. Ali, "Efficient Iris Image Recognition System Based on Machine Learning Approach," *Iraqi Journal of Computers, Communications, Control & Systems Engineering*, vol. 23, no. 3, pp. 104–114, 2023, https://doi.org/10.33103/uot.ijccce.23.3.9.

[42] T. Saidani, "Deep Learning Approach: YOLOv5-based Custom Object Detection," *Engineering, Technology & Applied Science Research*, vol. 13, no. 6, pp. 12158–12163, Dec. 2023, https://doi.org/10.48084/etasr.6397.

[43] R. Rajamohanan and B. C. Latha, "An Optimized YOLO v5 Model for Tomato Leaf Disease Classification with Field Dataset," *Engineering, Technology & Applied Science Research*, vol. 13, no. 6, pp. 12033–12038, Dec. 2023, https://doi.org/10.48084/etasr.6377.

[44] E. R. V. Reddy and S. Thale, "A Novel Efficient Dual-Gate Mixed Dilated Convolution Network for Multi-Scale Pedestrian Detection," *Engineering, Technology & Applied Science Research*, vol. 13, no. 6, pp. 11973–11979, Dec. 2023, https://doi.org/10.48084/etasr.6340.